AAPS PharmSciTech, Vol. 14, No. 1, March 2013 (© 2012)
DOI: 10.1208/s12249-012-9913-1

Research Article

Self-Associated Submicron IgG1 Particles for Pulmonary Delivery: Effects of Non-ionic Surfactants on Size, Shape, Stability, and Aerosol Performance

Asha R. Srinivasan[1] and Sunday A. Shoyele[2,3]

Received 12 April 2012; accepted 7 December 2012; published online 20 December 2012

Abstract. The ability to produce submicron particles of monoclonal antibodies of different sizes and shapes would enhance their application to pulmonary delivery. Although non-ionic surfactants are widely used as stabilizers in protein formulations, we hypothesized that non-ionic surfactants will affect the shape and size of submicron IgG particles manufactured through precipitation. Submicron particles of IgG1 were produced by a precipitation process which explores the fact that proteins have minimum solubility but maximum precipitation at the isoelectric point. Non-ionic surfactants were used for size and shape control, and as stabilizing agents. Aerosol performance of the antibody nanoparticles was assessed using Andersen Cascade Impactor. Spinhaler® and Handihaler® were used as model DPI devices. SEM micrographs revealed that the shape of the submicron particles was altered by varying the type of surfactant added to the precipitating medium. Particle size as measured by dynamic light scattering was also varied based on the type and concentration of the surfactant. The surfactants were able to stabilize the IgG during the precipitation process. Polyhedral, sponge-like, and spherical nanoparticles demonstrated improved aerosolization properties compared to irregularly shaped (>20 μm) unprocessed particles. Stable antibody submicron particles of different shapes and sizes were prepared. Careful control of the shape of such particles is critical to ensuring optimized lung delivery by dry powder inhalation.

KEY WORDS: aerosols; monoclonal antibodies; non-ionic surfactants; pulmonary delivery; submicron particles.

INTRODUCTION

Monoclonal antibodies (mAbs) are gradually emerging as one of the most important therapeutic agents in medicine. However, because they are poorly absorbed across biological membranes, they have been generally delivered intravenously (1,2). The parenteral route has several disadvantages, including patient discomfort, potential high cost, and the risk of needle-stick injuries (3–5). The pulmonary route offers an excellent alternative especially for mAbs targeted towards local lung diseases. mAbs such as bevacizumab, anatumomab, benralizumab, enokizumab, mitumomab, oxelumab, and palivizumab have gained FDA approval for the treatment of lung diseases such as asthma, lung cancers, and respiratory syncytial virus infection.

Submicron particles in pulmonary drug delivery may offer many advantages such as: (1) potentially allowing access to alveolar tissue, (2) an achievement of enhanced solubility of the drug than its aqueous solubility, (3) decreased incidence of side effects, (4) improved patience compliance, and (5) the potential of drug internalization by cells (6–8).

Currently, monoclonal antibodies are unable to benefit fully from the unique advantages offered by submicron particles in pulmonary drug delivery, mainly because of their labile molecular structure. The higher order structures of proteins, i.e., secondary, tertiary, and sometimes quaternary structures are stabilized by weak physical interactions such as hydrogen bonding, electrostatic attraction, van der Waal force, and hydrophobic interaction rather than the stronger covalent bond (5). Antibodies are therefore susceptible to various stresses involved in the fabrication of submicron particles. Presently, submicron particulate systems used in drug delivery include: polymer-based drug carriers (including polymeric nanospheres, polymeric micelles, and dendrimers), liposomes, viral nanoparticles, and carbon tubes (9). The processes involved in the fabrication of these particles often lead to degradation and sometimes loss of biological activity in the protein (10–12). Further, some materials used to formulate these particles may have toxic effects and may not be viable for the development of therapeutic proteins (13,14).

There is therefore a need for newer fabrication technologies that could produce submicron particles of different sizes and shapes that could potentially enhance the pulmonary delivery of mAbs. We hypothesize that non-ionic surfactants will affect the shape and size of submicron IgG particles manufactured through precipitation.

[1] Department of Pharmaceutical Sciences, School of Pharmacy, Thomas Jefferson University, 130 South 9th Street, Edison Building, Suite 1540, Philadelphia, Pennsylvania 19107, USA.
[2] Department of Pharmaceutical Sciences, School of Pharmacy, Thomas Jefferson University, 901 Walnut Street, Philadelphia, Pennsylvania 19107, USA.
[3] To whom correspondence should be addressed. (e-mail: sunday.shoyele@jefferson.edu)

In this work, using IgG1 antibody as a model, an antibody precipitation technique to produce submicron particles was developed by exploring the fact that proteins have minimum solubility but maximum precipitation at the isoelectric point (15,16). The effects of non-ionic surfactants Tween 80, Tween 20, and Brij 97 on the size, shape, and stability of the particles were investigated using analytical techniques such as dynamic light scattering (DLS), scanning electron microscopy (SEM), size-exclusion high-performance liquid chromatography (SE-HPLC), and circular dichroism (CD). It has been previously reported that the molecular structure of surfactants does affect the self-assembly pattern of nanostructures (17,18). It was on that premise that we investigated the effects of non-ionic surfactants on the particle size and morphology of IgG nanoparticles produced by precipitation.

The effects of particles shape and size on aerosol performance of these submicron particles were investigated using Andersen Cascade Impactor (ACI) with both Handihaler® and Spinhaler® as model DPI devices.

EXPERIMENTAL SECTION

Materials

Human polyclonal immunoglobulin G1 (IgG1) was supplied in an excipient-free lyophilized form by Equitech-Bio, Texas, USA. Polysorbate 80 (Polyoxyethylene (80) sorbitan monooleate), polysorbate 20 (Polyoxyethylene (19) sorbitan monolaurate), and Brij 97 (polyethylene glycol monooleyl ether) were supplied by Sigma-Aldrich, Saint Louis, Missouri. All other excipients and reagents were of reagent grades and were purchased from Fisher Scientific, Pittsburgh, Pennsylvania.

Methods

Manufacture of Protein Nanoparticles

Submicron particles were produced by dissolving different concentrations of the excipient-free human polyclonal IgG1 in 0.01 N HCl containing different concentrations of polysorbate 80 (Tween 80), polysorbate 20 (Tween 20), or Brij 97. Surfactant-free IgG dissolved in 0.01 N HCl was used as a control. The concentrations of IgG used were 5, 7.5, and 10 mg/mL, respectively. The mixture was then slowly titrated with 0.1 N NaOH to bring the pH of the mixture to 7 which is the iso-electric point of human IgG (as provided by the suppliers) while continuously mixing on a magnetic stirrer. At the iso-electric point, the mixture became turbid suggesting the precipitation of IgG particles. The colloidal suspension was then centrifuged using a microcentrifuge at 6500 RPM for 5 min. The supernatant was decanted and the pellet formed rinsed with double distilled deionized water in order to remove any unprecipitated IgG and unattached surfactant micelles.

Lyophilized samples were prepared by resuspending the particles in water by vortexing. The suspended particles were then snap-frozen using liquid nitrogen before being loaded into freeze dryer (Labconco Freezone 4.6, Missouri). Lyophilization was performed for 24 h. As control experiment, various concentrations of the surfactants used in the precipitation process were dissolved in 0.01 N HCl and titrated to pH 7 using 0.1 N NaOH. These were then used as controls in all the analytical procedures.

Percentage Yield of Nanoparticles

The percentage yield of submicron particles produced from the precipitation process was determined by taking samples from the supernatant following centrifugation and analyzing for protein content using UV absorption at 280 nm. Percentage yield was calculated as:

$$\text{Total amount of IgG} - \text{unprecipitated IgG}/\text{total amount of IgG} \times 100$$

Particle Size Analysis by Dynamic Light Scattering

The particle size analysis (by intensity) of the particles was performed by dynamic light scattering using Zetasizer Nano ZS (Malvern, UK). The pellets formed after centrifugation were thoroughly rinsed and resuspended in deionized water. The samples were then sonicated for approximately 5 min. Intensity autocorrelation was measured at a scattering angle (θ) of 173° at 25°C. The control samples (surfactants alone) described in the "Methods" section were also analyzed for particle size to see if the presence of micelles was interfering with the measurement. The Z-average and polydispersity index (PDI) were recorded in triplicate.

Scanning Electron Microscopy

The morphology of the manufactured particles and the unprocessed IgG was observed by scanning electron microscopy using the Zeiss Supra 50VP system (Zeiss, Germany). Powders were mounted onto aluminum stubs using double-sided adhesive tape and were made electrically conductive by coating in a thin layer of gold. The coated samples were then examined under a microscope operated at an acceleration voltage of 5 kV.

Protein Content by Absorbance at 280 nm

The IgG content in the particles formed was determined by constructing a standard calibration curve with unprocessed IgG with concentrations ranging from 0 to 3 mg/mL in 0.1 M acetate buffer pH 5. The UV absorbance of these solutions was measured at 280 nm. One mg/mL solutions of the dissolved particles were prepared and their "actual" concentrations determined by UV spectroscopy using the constructed calibration curve. IgG was determined as a percentage ratio of the "actual" concentrations to the theoretical concentrations (1 mg/mL). The experiment was repeated in triplicate for each sample. This was found to vary between 92% and 101%.

IgG Specific Binding Activity

ELISA was performed using a human IgG quantitation kit from Bethyl Laborotories Inc (Texas). Briefly, human IgG samples were reconstituted in 0.1 M acetate buffer (pH 5) at

250 ng/mL and were captured by the anti-human IgG antibody, which was pre-coated on the surface of in the microtiter wells following incubation for 60 min. Any unbound protein was washed off four times with the wash buffer. Biotinylated detection antibody was then added to the wells to bind to the captured human IgG and incubated at room temperature. After washing, 100 μL of horseradish peroxidase was then added to catalyze the colorimetric reaction with the chromogenic substrate 3, 3′, 5, 5′- tetramethylbenzidine. The reaction produced a blue-colored product in dark, which turned yellow when the reaction was terminated by the addition of dilute sulfuric acid. The absorbance of the yellow product was measured at 450 nm using a SpectraMax 340 (Molecular Devices, Sunnyvale, California). IgG standard curve was used in the 500–0.69-ng/mL range and was prepared by diluting the stock solution (500 ng/mL) with the dilution buffer provided by the supplier. Each sample was assayed three times (n=3), and all reactions were carried out at room temperature.

SE-HPLC

SE-HPLC was performed using an Alliance HPLC System, Waters 2695 separation module (Waters, Massachusetts, USA) combined with a Waters 2998 Photodiode Array Detector. A TSK Gel 3000 SWXL column (300× 7.8 mm; Tosoh Corporation, Ohio, USA) was used. Twenty microliters of IgG, dissolved in 0.1 M acetate buffer (pH 5) at 1 mg/mL, was injected, and separation was performed at a flow rate of 0.5 mL/min using 0.2 M sodium phosphate (pH 6.0) as the mobile phase. UV detection was performed at 214 nm. Chromatograms were recorded using the Empower Pro® software. The control samples (surfactants alone) described in the "Methods" section were also analyzed to see whether they interfere with the UV detection at 214 nm.

Far-UV Circular Dichroism Spectroscopy

CD measurements were performed with Jasco J-810 Spectropolarimeter (Jasco, Maryland, USA) operating at 20°C using 0.5 mg/mL of reconstituted solutions of IgG particles in acetate buffer. CD spectra were obtained in the far UV region (260–190 nm) using a quartz cell of 0.1 path length in order to probe the stability of the secondary structure of the manufactured particles. A scanning speed of 50 nm/min with a 0.5-s response time was applied followed by five accumulations for each sample. The experiment was repeated in triplicate for each sample. Surfactants dissolved in the acetate buffer at corresponding concentrations were used as blanks. Signals from blanks were subtracted from sample signals. The CD signals were converted to mean residue weight ellipticity. The percent estimate of the secondary structure retained was predicted using the K2D2 software.

In Vitro Deposition Studies Using the Andersen Cascade Impactor

The *in vitro* deposition patterns of the IgG particles were assessed using the eight-stage ACI (Copley Scientific, Nottingham, UK) as previously described (20) and according to USP, 2008 specifications (19). The flow rate (Q) through the ACI was set to 30 L/min using a flow meter model DFM2000 (Copley Scientific, Nottingham. UK). The pressure drop was set at 4 kPa. A 4-L inspiration volume was achieved by setting the timer so that t=[4×60/Q]s.

Using both Handihaler® (Boehringer Ingelheim, Germany) and Spinhaler® (Fison Pharmaceuticals, UK) as model devices, IgG powders containing an equivalent of 1 mg IgG were filled into the respective capsules before being loaded into the devices. The content of the capsule was then sampled by the ACI before collection of the plates on each stage and washing with 0.1 M acetate buffer pH 5. For each formulation, a total of six capsules were sampled. The content of IgG on each plate was quantified by UV absorption at 280 nm. The recovered dose was calculated as the total amount of drug recovered from the device, capsule, and the eight-stage impactor.

A table of cumulative mass% (as percentage of the total recovered emitted dose) *versus* effective cutoff diameter for each stage of the impactor was constructed. Fine particle fraction (FPF) was defined as the amount of IgG particles with aerodynamic diameter <5 μm. Analyses were run in triplicate and the data expressed as mean ± standard deviation.

RESULTS

Percentage Yield of Nanoparticles

The yields from all the preparations were approximately 85% irrespective of the type of the surfactant and the concentration of IgG in the precipitating medium.

Particle Size Analysis

DLS data in Table I reveal that the particles produced using this technology were in a size ranging from approximately 90 to 800 nm. Changes in the sizes of the particles were observed based on the type and concentration of the surfactant used. Table I reveals that the highest diameter (average of 795.7 nm) was produced by particles precipitated from the surfactant-free 5 mg/mL IgG solution (negative control). Upon the addition of Tween 80 to the precipitating medium, a concentration-dependent variation in size was observed. The smallest particles precipitated in the presence of Tween 80 from 5 mg/mL solution was when 0.1% *w*/*v* Tween 80 was added to the precipitating solution (average of 181.9 nm), while the biggest particles were produced in the presence of 0.3% *w*/*v* Tween 80 (average of 265.3 nm).

A more or less concentration-dependent variation in particle size was also observed with Tween 20 in the precipitating solution. When 0.1% *w*/*v* Tween 20 was added to the precipitating medium, particles with average of 403.5 nm in diameter were produced. In the presence of 0.2% *w*/*v* Tween 20, the particle size increased to 493.7 nm. The particle size stayed at an average of 493 nm when the concentration of the Tween 20 added was increased to 0.3% *w*/*v*.

When the concentration of the IgG in the precipitating solution was increased to 7.5 mg/mL, a concentration-dependent variation in particle size was also observed when the nanoprecipitation was performed in the presence of Tween 80 (Table I). Table I reveals that as the

Table I. Particle Size Analysis by DLS for Particles Precipitated from IgG Solutions

Sample	5 mg/ml IgG solution		7.5 mg/ml IgG solution		10 mg/ml IgG solution	
	Particle diameter (nm)[a]	PDI[a]	Particle diameter (nm)[a]	PDI[a]	Particle diameter (nm)[a]	PDI[a]
Particles precipitated with 0.1% Tween 80	181.9±4.9	0.1±0.0	132.5±4.6	0.1±0.1	110.8±5.6	0.6±0.1
Particles precipitated with 0.2% Tween 80	220.7±3.7	0.1±0.2	151.8±34.2	0.1±0.1	131.9±4.1	0.6±0.0
Particles precipitated with 0.3% Tween 80	265.3±2.3	0.1±0.3	187.2±1.7	0.1±0.1	188.0±6.9	0.5±0.0
Particles precipitated with 0.1% Tween 20	403.5±1.4	0.2±0.0	171.6±6.0	0.2±0.1	106.5±1.4	0.5±0.0
Particles precipitated with 0.2% Tween 20	493.7±0.8	0.1±0.2	183.7±9.0	0.1±0.0	160.1±8.3	0.6±0.1
Particles precipitated with 0.3% Tween 20	493.1±4.5	0.1±0.0	197.5±11.2	0.1±0.0	185.4±2.4	0.5±0.1
Particles precipitated with 0.1% Brij 97	492.6±7.9	0.2±0.1	489.7±1.4	0.2±0.0	94.2±5.7	0.3±0.1
Particles precipitated with 0.2% Brij 97	522.1±2.0	0.1±0.0	558.5±6.5	0.1±0.0	187.6±0.7	0.4±0.1
Particles precipitated with 0.3% Brij 97	535.7±3.6	0.1±0.1	563.9±3.4	0.1±0.1	243.3±4.0	0.7±0.1
Particles precipitated without surfactant (negative control)	795.7±8.8	0.1±0.1	774.9±8.2	0.1±0.2	741.3±7.0	0.4±0.0

[a] Data presented as mean±SD, n=3

concentration of Tween 20 in the 7.5 mg/mL IgG solution increased, the size of the particles produced increased from an average of 171.6 to 197.5 nm. The size of nanoparticles precipitated from the 10 mg/mL IgG solution is shown in Table I.

Particle Morphology

A conspicuous effect of the type of surfactant present in the precipitating medium on the shape of the particles produced can be seen in the SEM images. The unprocessed IgG as received from the supplier were irregularly shaped as seen in Fig. 1 (scale bar, 20 μm). Particles precipitated from surfactant-free 5 mg/mL IgG looked spherical (Fig. 2). Spherical IgG particles were formed when Tween 80 was used in the precipitating medium (Fig. 3). Polyhedral IgG particles were formed from 5 mg/mL IgG when Tween 20 was in the precipitating medium (Fig. 4). Spongy IgG particles were formed when Brij 97 was used in the precipitating medium (Fig. 5).

IgG Specific Binding Activity

The specific binding affinity of the IgG in the particles was determined by ELISA. This procedure was adapted from a previously described method by Dani *et al.* (21). Figures 6, 7, and 8 show the percentage specific binding activity retained by the IgG in the particles as fraction of the unprocessed IgG. Particles precipitated from surfactant-free IgG solutions retained the lowest binding activity in comparison to particles precipitated from the corresponding surfactant-containing solutions. The binding affinity retained by IgG in particles precipitated from surfactant-free (negative control) 5 mg/mL IgG solution was approximately 70% (Fig. 6). However, particles precipitated from corresponding IgG solutions containing 0.1%, 0.2%, and 0.3% Tween 80 retained approximately 109%, 108%, and 106% binding activity, suggesting that the presence of the Tween 80 in the precipitating solutions contributed to the retention of binding activity in the IgG particles. Similar trends were observed in the particles precipitated from solutions containing Tween 20 and Brij 97 (Figs. 7 and 8). It was interesting

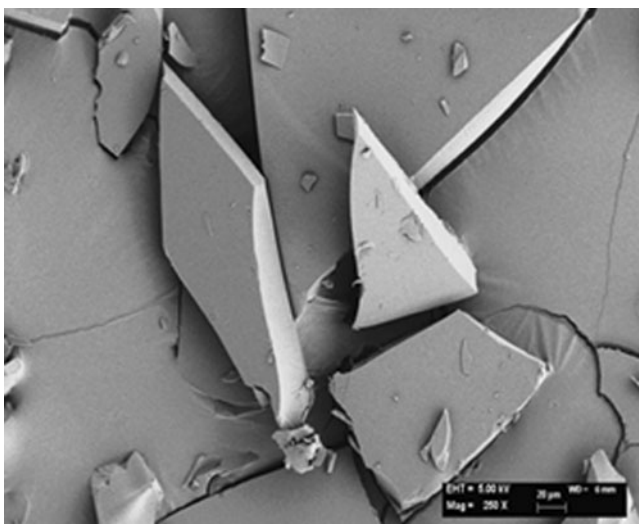

Fig. 1. SEM micrograph of the unprocessed IgG particles. *Scale bar* is 20 μm

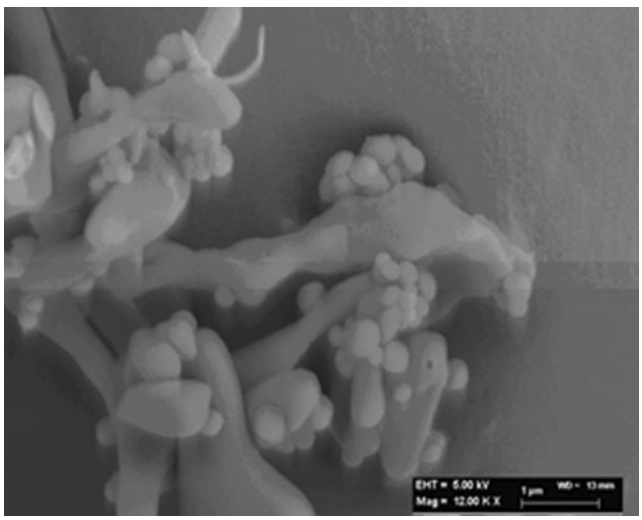

Fig. 2. SEM micrograph of IgG particles precipitated from 5 mg/ml solution in the absence of any surfactant. *Scale bar* is 1 μm

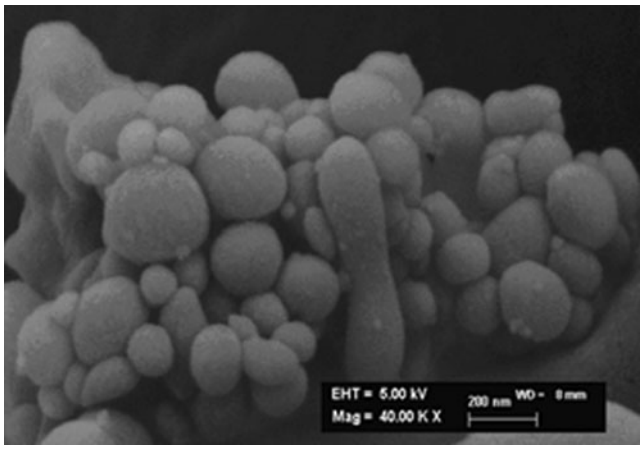

Fig. 3. SEM micrograph of IgG particles precipitated from 5 mg/ml solution in the presence of 0.1% *w/v* Tween 80. *Scale bar* is 200 nm

to see that for all the particles, irrespective of the concentrations and the type of surfactant used, particles precipitated from 5 mg/mL generally showed superior binding activity in comparison to the corresponding particles precipitated from 7.5 to 10 mg/mL. In Fig. 6, particles precipitated from the 5 mg/mL IgG solution containing 0.1% Tween 80 retained bioactivity of approximately 109%, while particles precipitated from corresponding solutions containing 7.5 and 10 mg/mL showed a retained binding activity of 90% and 80%, respectively.

SE-HPLC

The presence of monomers, soluble aggregates, and fragments in the reconstituted IgG particles was investigated using SE-HPLC. Figure 9 shows the SE-HPLC chromatogram of the unprocessed IgG. The peak at retention time of approximately 16 min represents the intact IgG monomer. The minor peaks at approximately 13 and 14 min suggest the presence of low levels of aggregates in the reconstituted unprocessed IgG. Peaks from all the reconstituted particles were similar to those seen in the unprocessed IgG.

The percentage monomer recovered from each nanoparticle formulation following reconstitution was determined and compared to that of the unprocessed IgG. Tables II, III, and IV show

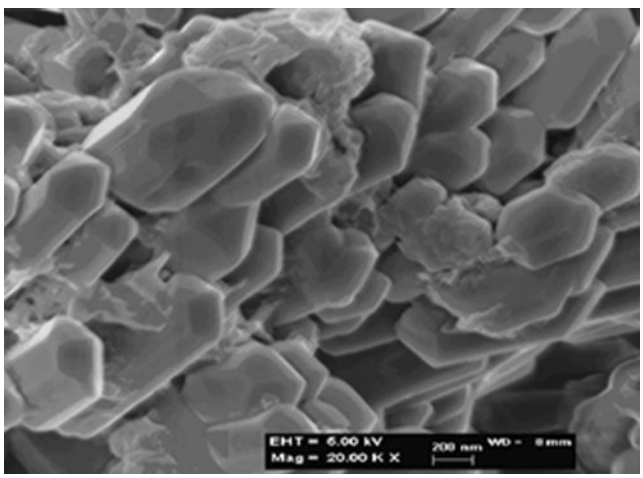

Fig. 4. SEM micrograph of IgG particles precipitated from 5 mg/ml solution in the presence of 0.1% *w/v* Tween 20. *Scale bar* is 200 nm

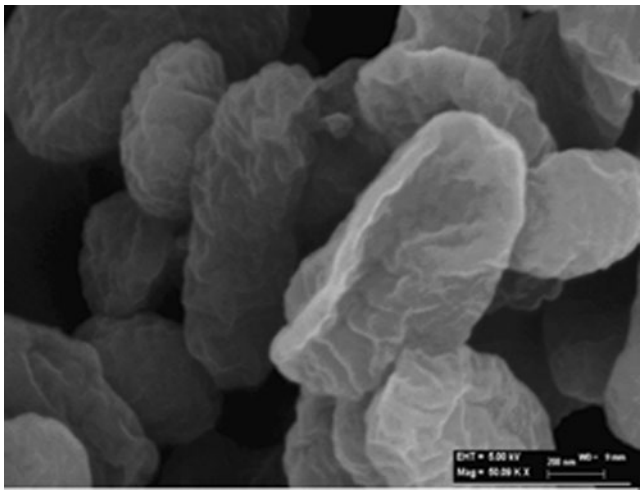

Fig. 5. SEM micrograph of IgG particles precipitated from 5 mg/ml solution in the presence of 0.1% *w/v* Brij 97. *Scale bar* is 20 nm

the percentages of the monomer recovered by SE-HPLC analysis. The percent monomer recovered from particles precipitated from 5 mg/mL IgG solutions ranged from 73% to 98% and 63% to 93% from 7.5 mg/mL solutions, while particles from 10 mg/mL IgG solutions had between 61% and 90% monomer recovery.

SE-HPLC data suggest that particles precipitated from 5 mg/mL IgG solutions had superior monomer recovery in comparison to the corresponding particles precipitated from 7.5 to 10 mg/mL solutions. Differences in concentrations of the surfactants did not seem to have an obvious effect on the percent monomer retained. However, the total relative recovery generally decreased as the concentration of the IgG solutions from which the particles were precipitated increased.

Far-UV Circular Dichroism Spectroscopy

The effects of the non-ionic surfactants Tween 80, Tween 20, and Brij 97 on the retention of the secondary structure of the IgG following the precipitation process were investigated using far-UV CD. Figure 10 reveals that the far-UV CD spectrum of the unprocessed IgG was characterized by a negative maximum at a wavelength of 218 nm and a positive maximum at 202 nm. These are characteristics typical for IgG because of their high β-sheet content (20–23). All the precipitated particles retained a β-sheet structure similar to the unprocessed IgG as seen in Fig. 10.

Table V shows the secondary structural contents of IgG particles generated from 5, 7.5, and 10 mg/mL IgG solutions. Data in Table V revealed that the unprocessed IgG contained approximately 41% β-sheet and 8% α-helix secondary structures. Following precipitation, most of the IgG in the particles precipitated from 5 mg/mL solutions retained similar secondary structure composition to that of the unprocessed IgG. However, major perturbations were found in IgG particles precipitated from 7.5 to 10 mg/mL IgG solutions.

Aerosol Performance Test Using ACI

Submicron particles generated from 5 mg/mL IgG solutions with or without 0.1% surfactant were compared to the unprocessed IgG particles in terms of aerosol performance. Table VI shows a summary of the aerodynamic particle size

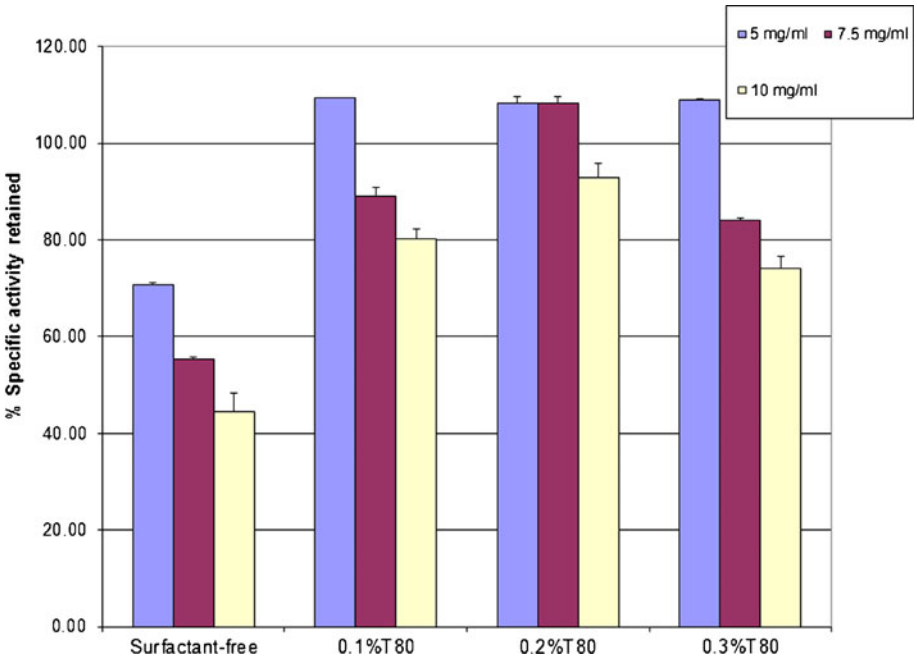

Fig. 6. Percent specific activity of IgG nanoparticles prepared from Tween 80-containing solutions as determined by ELISA as fraction of the starting activity prior to processing

metrics using both Handihaler® and Spinhaler® DPI devices. The FPF (<4.7 μm) of the unprocessed IgG particles was approximately 20% using Handihaler, while it was approximately 22% using Spinhaler. However, the surfactant-free particles had FPF of 53% using Handihaler. The FPF of these particles using Spinhaler (57%) was similar to that of the Handihaler, suggesting that the type of device used did not affect the aerosol performance of the nanoparticles. The SEM image of these surfactant-free particles in Fig. 2 reveals that they are predominantly spherical in shape. The particle size as measured by DLS was 515.7 nm, while the MMAD as measured by ACI was approximately 700 nm (0.7 μm) for both devices. Particles precipitated in the presence of 0.1% Tween 80 having similar spherical shape as the surfactant-free particles exhibited FPF of 55% using Handihaler and FPF of 53% using Spinhaler. The MMAD of the particle precipitated from 0.1 Tween 80 was 1.4 μm using Handihaler, while it was 1.9 μm using the Spinhaler. Particles precipitated in the presence of 0.1% Tween 80 and Brij 97 exhibited FPF of 68% and 67%, respectively, using Handihaler and 66% and 65%, respectively, using the Spinhaler. The MMAD of these particles were found to be similar as well, with both having MMADs of 0.8 μm using the Handihaler and 0.7 μm using the Spinhaler. Generally, there were similarities in the aerosol performance of the particles irrespective of the DPI device used. However, differences were found in the aerosol performance based on the type of particles.

DISCUSSION

Results presented above suggest that the precipitation process was able to produce submicron IgG particles of

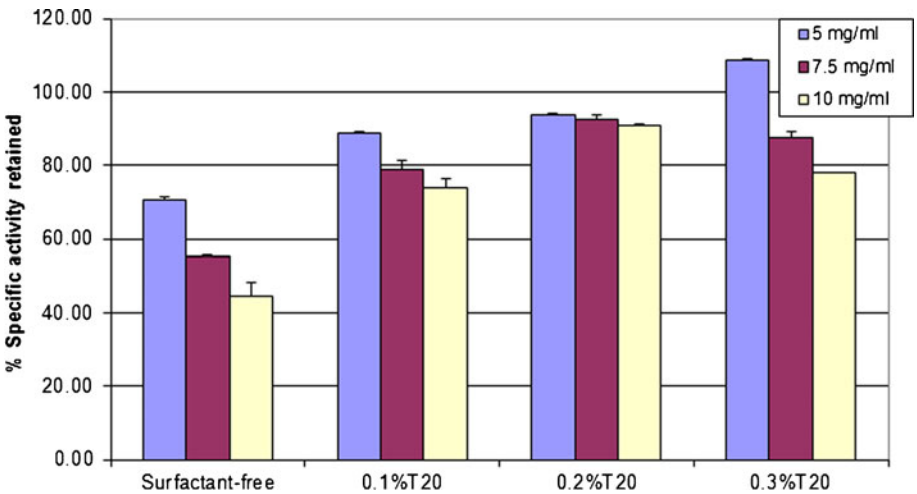

Fig. 7. Percent specific activity of IgG nanoparticles prepared from Tween 20-containing solutions as determined by ELISA as fraction of the starting activity prior to processing

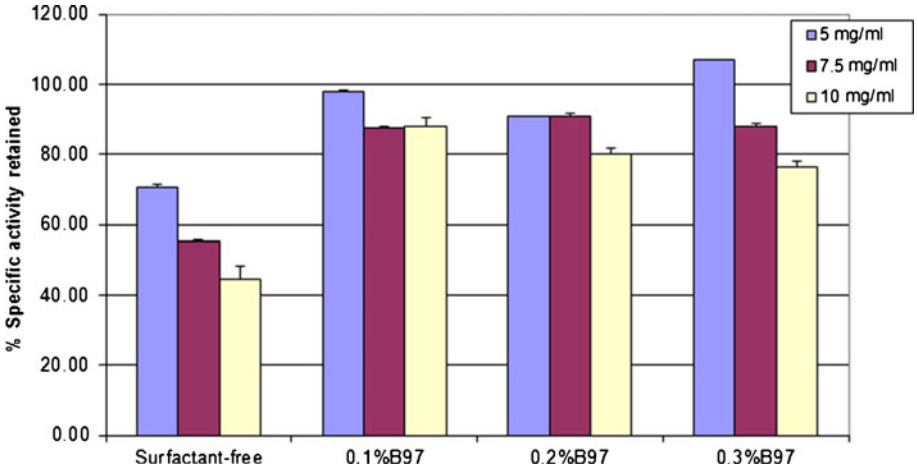

Fig. 8. Percent specific activity of IgG nanoparticles prepared from Brij 97-containing solutions as determined by ELISA as fraction of the starting activity prior to processing

different sizes and shapes by varying the concentration of the IgG in the precipitating solution as well as the type and concentration of the non-ionic surfactants. In this study, Tween 80, Tween 20, and Brij 97 were used for size and shape control during the precipitation process. They were also applied as protein stabilizing agents to help protect the IgG against the relatively harsh precipitating environment. The concentrations of the surfactants used were many folds higher than their respective critical micelle concentrations (CMC) in water which are 0.0017%, 0.0075%, and 0.029% for Tween 80, Tween 20, and Brij 97, respectively. Non-ionic surfactants have been well documented as effective stabilizing agents for proteins (24–26).

Generally, a surfactant concentration-dependent increase in particle size was observed for all particles. Another fascinating trend that was observed was the general decrease in the

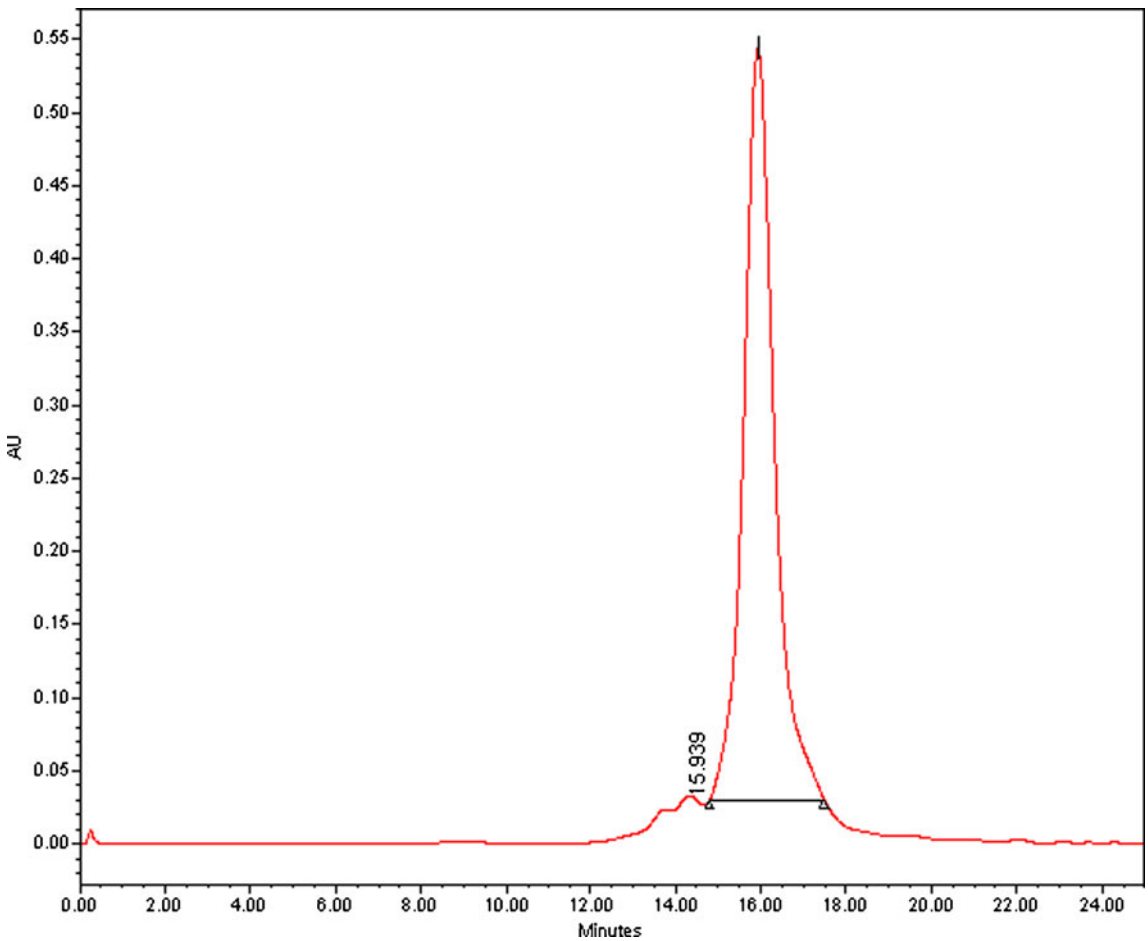

Fig. 9. SE-HPLC chromatogram of the unprocessed IgG solution (positive control)

Table II. SE-HPLC Analysis of Reconstituted IgG Nanoparticles Produced from 5 mg/ml Solutions

Sample	% Monomer[a]	% Dimer[a]	% HMW[a]	% Fragment[a]	% Relative recovery[b]
Unprocessed IgG	98.2±0.1	0.9±0.1	0.9±0.1	0.0	100±0.0
Particles precipitated without surfactant (negative control)	72.6±0.2	8.4±0.3	6.1±0.2	14.3±0.2	89.2±0.4
Particles precipitated with 0.1% Tween 80	98.4±0.2	0.6±0.2	0.8±0.2	0.2±0.1	96.6±0.2
Particles precipitated with 0.2% Tween 80	96.2±0.3	1.2±0.3	1.8±0.4	0.7±0.2	97.1±0.2
Particles precipitated with 0.3% Tween 80	96.8±0.1	1.1±0.2	1.7±0.3	0.9±0.3	96.8±0.3
Particles precipitated with 0.1% Tween 20	97.3±0.3	0.9±0.2	1.1±0.2	0.7±0.2	98.2±0.2
Particles precipitated with 0.2% Tween 20	96.9±0.2	1.0±0.3	1.7±0.4	0.7±0.3	98.2±0.3
Particles precipitated with 0.3% Tween 20	97.4±0.2	0.8±0.1	0.9±0.4	0.9±0.2	98.8±0.4
Particles precipitated with 0.1% Brij 97	98.2±0.1	0.9±0.2	0.6±0.2	0.6±0.2	97.3±0.3
Particles precipitated with 0.2% Brij 97	96.6±0.3	1.1±0.2	1.6±0.2	0.2±0.3	98.1±0.2
Particles precipitated with 0.3% Brij 97	97.2±0.1	1.0±0.2	0.9±0.1	0.8±0.2	97.6±0.2

[a] Data presented as mean±SD, n=3
[b] Relative recovery=area under the curve for dissolved nanoparticle/area under the curve for the unprocessed

size of the particles as the concentration of the IgG in the precipitating medium increased from 5 to 10 mg/mL. This surfactant concentration-dependent increase in particle size exhibited by the particles could be attributed to an increasing influence of the surfactant in the self-association of the IgG molecules during the precipitation process. Previous report has shown that non-ionic surfactants interact with polymers (proteins are biopolymers) during self-association, especially when the surfactant is used at concentrations above its CMC. The presence of hydrophobic groups on the protein enhances the interaction between the protein and non-ionic surfactants (27).

We propose that, because surfactants have a natural tendency to self-assemble into micelles at concentrations above the CMC, they probably aid the self-association of the IgG by including the IgG in the self-assembly process since they exhibit hydrophobic interaction with the IgG. Further, the IgG may be incorporated inside the micelles as a particle and therefore take the shape of the micelles.

SEM micrographs (Figs. 1, 2, 3, 4, and 5) showed that the morphology of the particles produced by the precipitation technology may be influenced by the type of surfactant incorporated in the precipitating solution. The change in particle shape may be attributed to the differences in the molecular structures of the surfactants used. It has been previously reported that the self-assembly pattern of nanostructures is influenced by the molecular structure of surfactants applied in the fabrication process, although the mechanisms through which this occurs are not yet fully understood (17,18).

Interestingly, the particle size data as provided by DLS seem marginally different from the size of the particles visually observed from the SEM micrographs. This is because the DLS measures the hydrodynamic diameter due to the solvent effect (28), while SEM only gives an estimate of the particle size and is not always accurate. Further, many biological compounds (e.g., liposomes and proteins) and engineered polymers (e.g., dendrimers) are invisible to SEM without heavy-metal staining procedures because these compounds do not deflect an electron beam sufficiently. For these "soft" particles, SEM does not always provide a relevant measure of particle size (29).

It is important that the conformational structure of the IgG is maintained after the reconstitution of the particles in a buffer (if needed), or after going into dissolution in the body. It is also expected that these particles would go into dissolution at an acidic pH due to its isoelectric point (pI). It is well established that major perturbations in the conformational structure of a protein often lead to a reduction or even a loss of the biological activity of the protein (5,21,30,31). Further, soluble aggregates in protein formulations are undesirable

Table III. SE-HPLC Analysis of Reconstituted IgG Nanoparticles Produced from 7.5-mg/ml Solutions

Sample	% Monomer[a]	% Dimer[a]	%HMW[a]	% Fragment[a]	% Relative recovery[b]
Unprocessed IgG	98.2±0.1	0.9±0.1	0.9±0.1	0.0	100±0.0
Particles precipitated without surfactant (negative control)	63.3±0.2	14.9±0.2	10.2±0.3	12.2±0.2	86.1±0.3
Particles precipitated with 0.1% Tween 80	92.4±0.3	4.6±0.3	3.2±0.2	0.2±0.2	93.3±0.3
Particles precipitated with 0.2% Tween 80	93.2±0.3	4.2±0.1	3.6±0.3	0.2±0.1	94.3±0.2
Particles precipitated with 0.3% Tween 80	93.1±0.2	4.0±0.3	3.8±0.2	0.1±0.3	93.7±0.3
Particles precipitated with 0.1% Tween 20	92.8±0.3	3.4±0.2	3.0±0.4	0.4±0.2	94.2±0.4
Particles precipitated with 0.2% Tween 20	92.3±0.2	3.0±0.3	3.7±0.3	0.5±0.2	95.1±0.1
Particles precipitated with 0.3% Tween 20	92.1±0.3	3.2±0.2	3.6±0.2	0.3±0.2	94.2±0.2
Particles precipitated with 0.1% Brij 97	93.2±0.2	4.0±0.3	3.2±0.2	0.3±0.1	93.1±0.3
Particles precipitated with 0.2% Brij 97	92.1±0.3	3.1±0.2	3.9±0.2	0.7±0.1	92.8±0.3
Particles precipitated with 0.3% Brij 97	91.8±0.2	3.9±0.2	4.0±0.3	0.6±0.3	93.1±0.4

[a] Data presented as mean±SD, n=3
[b] Relative recovery=area under the curve for dissolved nanoparticle/area under the curve for the unprocessed

Table IV. SE-HPLC Analysis of Reconstituted IgG Nanoparticles Produced from 10-mg/ml Solutions

Sample	% Monomer[a]	% Dimer[a]	%HMW[a]	% Fragment[a]	% Relative recovery[b]
Unprocessed IgG	98.2±0.1	0.9±0.1	0.9±0.1	0.0	100±0.0
Particles precipitated without surfactant (negative control)	61.2±0.2	15.8±0.3	11.8±0.3	13.5±0.2	80.2±0.2
Particles precipitated with 0.1% Tween 80	89.6±0.2	5.8±0.3	3.1±0.2	1.1±0.2	88.3±0.3
Particles precipitated with 0.2% Tween 80	90.2±0.1	4.2±0.3	4.2±0.3	1.2±0.1	89.1±0.2
Particles precipitated with 0.3% Tween 80	91.3±0.3	4.3±0.2	4.4±0.3	0.2±0.2	88.1±0.3
Particles precipitated with 0.1% Tween 20	89.3±0.2	5.7±0.3	4.2±0.2	0.9±0.3	89.2±0.2
Particles precipitated with 0.2% Tween 20	90.8±0.3	4.2±0.2	4.1±0.3	0.7±0.2	90.1±0.3
Particles precipitated with 0.3% Tween 20	90.2±0.3	4.1±0.3	4.4±0.2	0.5±0.2	91.8±0.2
Particles precipitated with 0.1% Brij 97	88.3±0.2	5.8±0.2	5.5±0.1	0.2±0.2	90.1±0.3
Particles precipitated with 0.2% Brij 97	89.1±0.3	5.9±0.3	5.4±0.3	0.4±0.3	92.1±0.2
Particles precipitated with 0.3% Brij 97	89.2±0.2	5.7±0.1	5.6±0.2	0.2±0.3	91.9±0.3

[a] Data presented as mean±SD, n=3
[b] Relative recovery=area under the curve for dissolved nanoparticle/area under the curve for the unprocessed

because of their immunogenicity (32–34). SE-HPLC was used to investigate the presence of soluble aggregates as well as fragments in the reconstituted IgG particles. The particles were reconstituted at pH 5 and not 7 since proteins have minimum solubility at their pI (15,16). Further, should there be a need for the nanoparticles to be reconstituted before application; slightly acidic buffers would be the solvents of choice due to the pI of the antibody. It is therefore important that the IgG is stable at this pH following reconstitution. As shown in Fig. 9, the unprocessed IgG (positive control) showed a prominent peak at approximately 16 min indicating predominantly the presence of monomeric IgG.

Particles precipitated from 10-mg/mL solutions generally had lower monomer contents in comparison to the particles precipitated from corresponding 5- and 7.5-mg/mL solutions. This could be attributed to the relatively higher concentration of IgG in the precipitating solution. These results are consistent with the report previously published by Dani and coworkers (21). Due to the increased proximity due to increased concentration, partially unfolded IgG molecules would have increased tendency to aggregate.

Surfactant-free IgG particles (negative control) generally produced high levels of fragments. Fragments formation may be attributed to the hydrolysis of the peptide bonds by the HCl that was used to precipitate the particles (35–37). Following the addition of the non-ionic surfactant to the precipitating solution, particles formed were more stable (Tables II, III, and IV) in comparison to the particles precipitated from the surfactant-free solution. These results suggest that the non-ionic surfactants included in the precipitating solutions may help to stabilize the IgG during the precipitation process. The stabilization may be attributed to the hydrophobic interaction with protein molecules (24,38,39). It is also possible that the surfactants form micelles around the IgG molecules during the precipitation process, thereby protecting them from the harsh precipitating environment.

Binding activity data presented in Figs. 6, 7, 8, and 9 seem to be consistent with the SE-HPLC data. Figure 6 reveals that

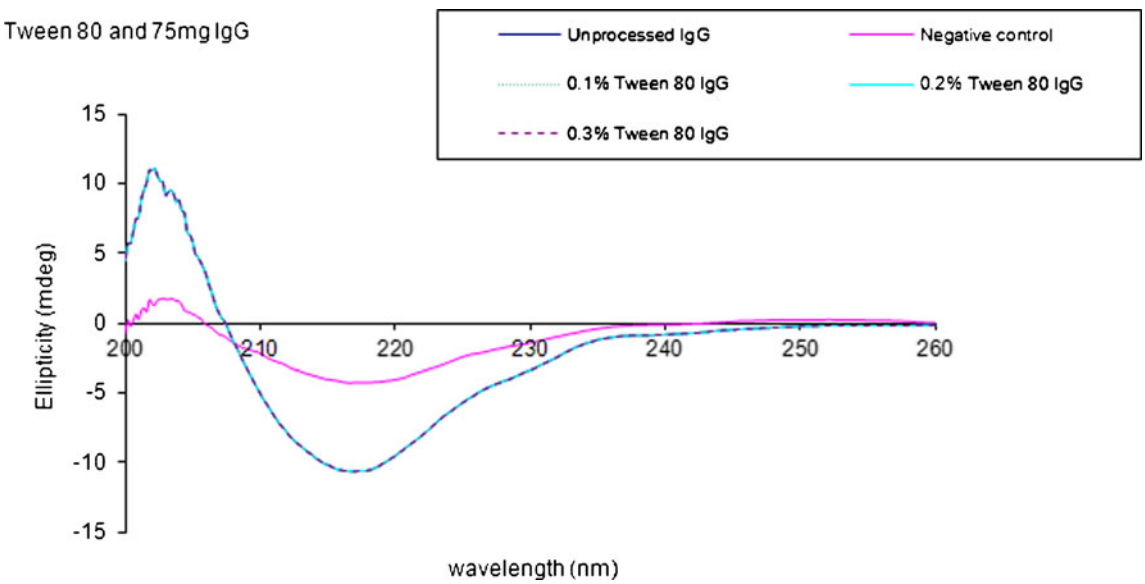

Fig. 10. Far-UV CD spectra from nanoparticles generated from 7.5-mg/ml IgG solutions in the presence of Tween 80. Negative control represents the surfactant-free IgG formulation

Table V. Estimated Secondary Structure Contents of IgG Nanoparticles as Measured by CD

Sample	5 mg/ml IgG solution		7.5 mg/ml IgG solution		10 mg/ml IgG solution	
	%Alpha helix	%Beta sheet	%Alpha helix	%Beta Sheet	%Alpha helix	%Beta sheet
Unprocessed IgG	7.7±0.2	41.3±9.5	7.7±0.2	41.3±9.5	7.7±0.2	41.3±9.5
Particles precipitated with 0.1% Tween 80	7.6±2.9	41.2±5.4	3.7±0.0	44.5±0.0	8.4±0.2	35.3±1.9
Particles precipitated with 0.2% Tween 80	7.7±2.1	42.3±0.1	11.8±1.5	43.9±1.3	8.2±0.2	23.6±2.5
Particles precipitated with 0.3% Tween 80	7.7±1.4	42.2±0.1	2.8±0.0	51.1±0.0	8.1±0.1	23.4±1.1
Particles precipitated with 0.1% Tween 20	7.4±4.8	41.5±2.0	3.6±0.1	45.4±1.5	8.16±0.0	24.1±0.1
Particles precipitated with 0.2% Tween 20	7.0±0.6	41.9±2.3	9.6±1.4	26.8±4.0	8.0±0.1	22.1±0.1
Particles precipitated with 0.3% Tween 20	4.2±0.0	45.6±2.7	9.6±1.3	29.8±7.8	13.8±2.9	27.3±1.5
Particles precipitated with 0.1% Brij 97	7.2±2.0	41.1±3.1	10.8±0.8	38.7±2.3	10.5±0.1	29.1±0.1
Particles precipitated with 0.2% Brij 97	7.8±1.4	44.5±4.0	9.7±1.3	25.6±1.4	8.02±0.1	22.1±0.1
Particles precipitated with 0.3% Brij 97	7.3±3.8	41.9±3.5	9.8±1.4	25.6±1.4	8.1±0.1	23.4±1.1
Particles precipitated without surfactant (negative control)	10.5±0.0	29.1±0.0	8.6±0.1	25.1±1.5	8.02±0.0	22.1±0.0

Tween 80 seems to improve the bioactivity of IgG in particles in comparison to the particles precipitated from the surfactant-free IgG solutions (negative control). Further, nanoparticles from 5-mg/mL solutions had superior binding activity to those precipitated from corresponding 7.5- and 10-mg/mL solutions (see Fig. 6, 7, 8, and 9). This trend was quite consistent for the other surfactants as shown in Figs. 7 and 8. The specific binding activity results suggest that the monomer contents of the reconstituted particles had a great impact on their binding activity.

The results obtained from reconstituted IgG particles are consistent with the published CD data for human IgG (19,23). K2D2 data in Table V suggest that the surfactants contributed to the retention of the secondary structure in the IgG nanoparticles. The particles precipitated from surfactant-free solutions irrespective of the concentration of the IgG showed major perturbations in their secondary structures. Generally, particles precipitated from 5-mg/mL IgG solutions had higher β-sheet contents in comparison to the corresponding particles precipitated from both 7.5- and 10-mg/mL solutions. We hypothesize that this was caused by the higher ratio of IgG to surfactants in these solutions of higher protein concentrations in comparison to the 5-mg/mL solution which obviously had lower ratio of IgG to surfactants in the respective solutions. Due to the relatively lower ratio of IgG to surfactants in the 5 mg/mL, more molecules of IgG were probably better protected by the surfactants than in the corresponding 7.5- and 10-mg/mL solutions suggesting that protein concentration is an important variable for ameliorating aggregation in this technology.

Table VI reveals the *in vitro* deposition patterns of IgG particles as analyzed by ACI using both Handihaler® and Spinhaler® DPI devices. Similar trends were observed for the aerosol deposition patterns of both devices. However, a shape-dependent difference in aerosol deposition pattern was observed. Previous report has shown that elongated and pollen-shaped particles tend to exhibit better flowability and higher FPF than spherical particles (40). This is because elongated particles have longer suspended time in the air and can travel further in the lung airways (40). Further, the sponge-like particles exhibited rough surfaces, and particles with rough surfaces tend to have improved flowability due to reduced van Der Waal forces because of reduced inter-particulate contact area (20). This improved flowability ultimately leads to enhanced aerosol performance (40).

CONCLUSIONS

Stable submicron IgG particles of different sizes and shapes were produced by a precipitation process using nonionic surfactants for shape and size control. Elongated and sponge-shaped particles were found to exhibit superior aerosol performance in comparison to spherical particles. Further work is ongoing to determine if this technology can be applied to other therapeutic monoclonal antibodies.

Table VI. Summary of the Aerodynamic Particle Size Distribution Metrics for IgG Nanoparticles Using Andersen Cascade Impactor (n=3, mean±SD)

Particles	Handihaler				Spinhaler			
	FPF (%)	MMAD (μm)	GSD	ED (%)	FPF (%)	MMAD (μm)	GSD	ED
Unprocessed IgG	20±4	8.1±0.4	3.2±0.2	97±2	22±2	8.5±0.3	2.2±0.3	95±3
Surfactant-free nano	53±3	0.7±0.2	3.1±0.1	85±3	57±4	0.7±0.3	3.2±0.1	89±3
0.1% Tween 80 nano	55±4	1.4±0.4	2.4±0.2	89±3	53±4	1.9±0.3	2.2±0.3	86±2
0.1% Tween 20 nano	68±3	0.8±0.2	2.7±0.3	91±2	66±2	0.7±0.1	3.1±0.2	90±4
0.1% Brij 97 nano	67±4	0.8±0.3	2.0±0.2	89±3	65±4	0.7±0.3	2.4±0.2	89±1

FPF fine particle fraction, *MMAD* mass median aerodynamic diameter from cascade impaction, *GSD* geometric standard deviation, *ED* emitted dose

ACKNOWLEDGMENTS

The authors would like to thank Thomas Jefferson University (TJU) for providing start-up grant for Dr. Shoyele. We would also like to thank the Kimmel Cancer Center of TJU for providing the CD instrument used for this work and Drexel University for the use of their SEM.

REFERENCES

1. Kegan L, Turner MR, Balu-lyer SV, Mager DE. Subcutaneous absorption of monoclonal antibodies: role of dose, site of injection and Injection volume on Rituximab pharmacokinetics in rats. Pharm Res. 2011. doi 10.1007/s11095-011-0578-3.
2. Roskos LK, Davis CG, Schwab GM. The clinical pharmacology of therapeutic monoclonal antibodies. Drug Dev Res. 2004;61:108–20.
3. Patton JS. Deep lung delivery of therapeutic protein. Chemtech. 1997;27:34–8.
4. Shoyele SA, Cawthorne S. Particle engineering techniques for inhaled biopharmaceuticals. Adv Drug Deliv Rev. 2006;58:1009–29.
5. Shoyele SA, Slowey A. Prospects of formulating proteins/peptides as aerosols for pulmonary drug delivery. Int J Pharm. 2006;314:1–8.
6. Mansour HM, Rhee Y-S, Wu X. Nanomedicine in pulmonary delivery. Int J Nanomedicine. 2009;4:299–319.
7. Sung JC, Pulliam BL, Edwards DA. Nanoparticles for drug delivery to the lungs. Trends Biotechnol. 2007;25:563–70.
8. Bailey MM, Berkland CJ. Nanoparticles formulation in pulmonary drug delivery. Med Res Rev. 2009;29:196–212.
9. Cho K, Wang X, Nie S, Chen ZG, Shin DM. Therapeutics nanoparticles for drug delivery in cancer. Clin Cancer Res. 2008;14:1310–6.
10. Peterson LK, Sackett CK, Narasimhan B. High throughput analysis of protein stability in polyanhydride nanoparticles. Acta Biomater. 2010;6:3873–81.
11. Kim KR, Ahn KY, Park JS, Lee KE, Jeon H, Lee J. Lyophilization and enhanced stability of fluorescent protein nanoparticles. Biochem Biophys Res Commun. 2011;408:225–9.
12. Son S, Lee WR, Joung YK, Kwom MK, Kim YS, Park KD. Optimized stability retention of a monoclonal antibody in PLGA nanoparticles. Int J Pharm. 2009;368:178–85.
13. Zhang K, Fang H, Chen Z, Taylor J-SA, Wooley KL. Shape effects of nanoparticles conjugated with cell-penetration peptides (HIV Tat PTD) on CHO cell uptake. Bioconjug Chem. 2008;19:1880–7.
14. Kleemann E, Neu M, Jekel N, Fink L, Schmehl T, Gessler T, Seeger W, Kissel T. Nano-carriers for DNA delivery to the lung based upon a TAT derived peptide covalently coupled to PEG-PEI. J Control Release. 2005;109:299–316.
15. Ingham KC. Precipitation of proteins with polyethylene glycol. In: Deutscher MP, editor. Guide to protein purification. San Diego: Academic; 1990. p. 301–6.
16. Ries-Kautt M, Ducruix A. Phase diagrams. In: Ducruix A, Giege R, editors. Cerystallization of nucleic acids and proteins. 1st ed. Oxford: Oxford University Press; 1992. p. 195–218.
17. Tummala NR, Alberto S. SDS surfactants on carbon nanotubes: aggregates morphology. ACS Nano. 2009;3:595–602.
18. Suttipon M, Tummala NR, Kitiyanan B, Alberto S. Role of surfactant molecular structure on self-assembly: aqueous SDBS on carbon nanotubes. J Phys Chem C. 2011;115:17286–96.
19. United States Pharmacopoeia (USP), United States Pharmacopoeia Convention Inc., USA, 2008.
20. Shoyele SA, Sivadas N, Cryan S-A. The effects of excipients and particle engineering on the biophysical stability and aerosol performance of parathyroid hormone (1–34) prepared as a dry powder for inhalation. AAPS PharmSciTech. 2011;12:304–11.
21. Dani B, Platz R, Tzannis ST. High concentration formulation feasibility of human immunoglobulin G for subcutaneous administration. J Pharm Sci. 2007;96:1504–17.
22. Hawe A, Kasper JC, Fries W, Jiskoot W. Structural properties of monoclonal antibody aggregates induced by freeze-thawing and thermal stress. Eur J Pharm Sci. 2009;38:79–87.
23. Doi E, Jirgensons B. Circular dichroism studies on the acid denaturation of gamma-immunoglobulin G and its fragments. Biochemistry. 1970;9:1066–72.
24. Pelton JT, McClean LR. Spectroscopic methods for analysis of protein secondary structure. Anal Biochem. 2000;277:167–76.
25. Bam NB, Cleland JL, Yang J, Manning MC, Carpenter JF, Kelley RF, Randolph TW. Tween protects recombinant human growth hormone against agitation-induced damage via hydrophobic interactions. J Pharm Sci. 1998;87:1554–9.
26. Andya JD, Maa YF, Costantino HR, Nguyen PA, Dasovich N, Sweeney TD. The effect of formulation excipients on protein stability and aerosol performance of spray-dried powders of a recombinant humanized anti-IgE monoclonal antibody. Pharm Res. 1999;16:350–8.
27. Hillgren A, Alden MA. A comparison between the protection of LDH during freeze thawing by PEG 6000 and Brij 35 at low concentrations. Int J Pharm. 2002;244:137–49.
28. Sivadasan K, Somasundaran P. Polymer-surfactant interactions and the association behavior of hydrophobically modified hydroxyethylcellulose. Colloids Surf. 1990;49:229–39.
29. Liv CG, Desai KGH, Chen XG, Park HJ. Linolenic acid-modified chitosan for formation of self-assembled nanoparticles. J Agric Food Chem. 2005;53:437–41.
30. Hall JB, Dobrovolskia MA, Patri AK, McNeil SE. Characterization of nanoparticles for therapeutics. Futur Med Nanomedicine. 2007;2(6):789–803.
31. Sviridov OV, Ermolenko MN, Cheikina AV, Martsev SP. Effect of structural changes in thyroxine-binding globulin on its biological activity and immunochemical properties. Biokhimiia. 1988;53:61–8.
32. Manning MC, Patel K, Borchardt RT. Stability of protein pharmaceuticals. Pharm Res. 1989;6:903–18.
33. Rosenberg AS. Effect of protein aggregates: an immunologic perspective. The AAPS Journal. 2006; 8(3) Article 59 (http://www.aaps.org). Accessed 3 Dec 2011.
34. Cleland J, Powell M, Shire SJ. The development of stable protein formulations: a close look at protein aggregation, deamidation and oxidation. Crit Rev Ther Drug Carrier Syst. 1993;10:307–77.
35. Hermeling S, Schellekens H, Crommelin DJ, Jiskoot W. Micelle associated protein in epoetin formulations: a risk factor for immunogenicity? Pharm Res. 2003;20:1903–7.
36. Schrier JA, Kenley RA, Williams R, Corcoran RJ, Kim Y, Northey RP, D'Augusta D, Hberty M. Degradation pathways for recombinant human macrophage colony-stimulating factor in aqueous solution. Pharm Res. 1993;10:933–44.
37. Kenley RA, Warne NW. Acid catalyzed peptide bond hydrolysis of recombinant human interleukin 11. Pharm Res. 1994;11:72–6.
38. Bond MD, Panek ME, Zhang Z, Wang D, Mehndiratta P, Zhao H, Gunton K, Ni A, Nedved ML, Burman S, Volkin DB. Evaluation of a dual-wavelength size exclusion HPLC method with improved sensitivity to detect protein aggregates and its use to better characterize degradation pathways of an IgG1 monoclonal antibody. J Pharm Sci. 2010;99:2582–97.
39. Tandon S, Horowitz PM. Detergent-assisted refolding of guanidinium chloride-denatured rhodanese—the effects of the concentration and type of detergent. J Biol Chem. 1987;262:4486–91.
40. Hassan MS, Lau RWM. Effect of particle shape on dry particle inhalation: study of flowability, aerosolization and deposition properties. AAPS PharmSciTech. 2009;10:1252–62.